

Chiral Perturbation Theory Calculations For S-wave π^0 production In pp Collision

E.Gedalin^{*}, A.Moalem[†] and L.Razdolskaya[‡]

Department of Physics, Ben Gurion University, 84105 Beer Sheva, Israel

Abstract

The total cross section for the $pp \rightarrow pp\pi^0$ reaction at energies close to threshold is calculated within the frame of a chiral perturbation theory. The tree and one loop diagrams up to chiral order $D = 2$ contributions are taken into account. The $L^{(0)}$ isoscalar-scalar part of t-channel two-pion exchange loop diagrams enhances the production amplitude strongly. The calculated cross section scale and energy dependence are very close to data.

13.75.Cs, 14.40.Aq, 25.40.Ep

Typeset using REVTeX

^{*}gedal@bgumail.bgu.ac.il

[†]moalem@bgumail.bgu.ac.il

[‡]ljuba@bgumail.bgu.ac.il

In two recent contributions [1,2], the cross section for the $pp \rightarrow pp\pi^0$ reaction at energies near threshold was calculated within the frame work of chiral perturbation theory (χ PT). Although χ PT accounts for all effects such as offshellness, unitarity and spontaneously broken chiral symmetry, the calculations of Refs. [1,2] underestimate the cross section data by a factor of 4-6. This stands in marked difference with the results from traditional one-boson exchange (OBE) model calculations, where contributions from heavy meson exchanges seem to resolve the discrepancy between predictions and data [3–5]. Particularly, by applying a covariant OBE model the production amplitude is found to be dominated by the exchange of a σ -meson, due to a strongly enhanced t-pole term [5]. It is the purpose of the present note to show that the failure of χ PT calculations [1,2] to reproduce data may not be due to limitations of theory but to inconsistencies in the way χ PT was applied to this process and, that including loop contributions properly may resolve the discrepancy between predictions and data.

A meson production in NN collisions necessarily involves large momentum transfers and, it is expected that loop diagrams describing short interactions may play an important role. The exchange of an effective isoscalar-scalar σ -meson simulates the exchange of two correlated pions and, to the extent a t-pole term dominates the process, there must exist equally important contributions from the isoscalar-scalar part of t-channel two-pion exchange loop diagrams. Clearly the existing χ PT formalism [6], [7], [8] already accounts for such contributions and there is no need to introduce them externally. Basically, for the same reasons the low energy χ PT coupling constants encode only resonance meson exchanges which describe short range interactions of the Goldstone bosons and nucleons.

A prominent feature of a production process is that the transferred four momentum q^2 is space like and rather large. At threshold $q^2 = -Mm$, where M and m are the masses of the nucleon and the meson produced. This has two important consequences. The first is that off mass-shell effects must be calculated exactly [1,2] because these may enhance strongly the contributions from diagrams involving large momentum transfer. In practice, for the $pp \rightarrow pp\pi^0$ reaction, the amplitude corresponding to one-pion exchange including one-loop

contributions, hereafter to be noted by $T(\pi^0 p \rightarrow \pi^0 p)$, becomes large due to offshellness. The second consequence is concerned with the χ PT expansion convergence. The χ PT expansion parameter is $q/M \sim q/(4\pi F)$. For low momentum transfer processes, $q \leq m$ the expansion parameter is small and contributions from loop diagrams are rather small so that their overall contributions to the transition amplitude is also small. For the $pp \rightarrow pp\pi^0$ reaction, however, the expansion parameter is relatively large [2], of the order $\sim \sqrt{m/M}$, and each of the Born, rescattering and one-loop diagrams terms is of the same order of magnitude, *i.e.*, m/M . Therefore, for the sake of consistency all three contributions must be taken into account. Formally, the chiral order D=1 Lagrangian coupling constants, c_1 , c_2 , c_3 , are determined from π N elastic scattering data analysis which accounts for one-loop contributions, and using these constants to calculate the cross section for the $pp \rightarrow pp\pi^0$ reaction would also require that these diagrams should not be neglected.

We follow Refs. [5,9,10] and write the transition operator for a production process, $NN \rightarrow NNB$, in the form,

$$\hat{T}_{23} = \hat{Z}_{33} \hat{M}_{23}^{(in)} \hat{X}_{22} \quad , \quad (1)$$

where $\hat{M}_{23}^{(in)}$ is the primary production operator which describes the transition from a two-nucleon state to a three-body state of two nucleon and a boson B, and \hat{Z}_{33} and \hat{X}_{22} are operators accounting for final state interactions (FSI) and initial state interactions (ISI) corrections, respectively. The $\hat{M}_{23}^{(in)}$ contains all possible inelastic interactions while \hat{Z}_{33} and \hat{X}_{22} involve elastic interactions only between particles in the exit and entrance channels. From a diagrammatic point of view, the operator $\hat{M}_{23}^{(in)}$ is the sum of all connected diagrams that begin with the two initial lines and end with the three final particle lines. The correction terms \hat{Z}_{33} and \hat{X}_{22} are the sum of all diagrams (both connected and disconnected) that can be formed from elastic scattering blocks. It is to be noted that while $\hat{M}_{23}^{(in)}$ involves large momentum transfer ($q^2 \sim -Mm$) the ISI and FSI correction factors involve small momentum transfers only. Accordingly, it is not possible to separate from the diagrams contributing to $\hat{M}_{23}^{(in)}$, sub-diagrams which involve initial or final particle elastic scattering only.

There exist, the so called reducible diagrams in the Weinberg's sense [11], with nucleons almost on the mass shell. These diagrams split into irreducible sub-diagrams by cutting such nucleon lines. Cohen et al. [2] apply a revised notion of irreducibility, where a sub-diagram is irreducible if it includes a small energy denominator $\sim m^2$ and irreducible otherwise. The reducible diagrams can be used to generate, by iterations, initial and final states wave functions. The χ PT amplitude can then be derived as an overlap integral of these functions and the irreducible term $\hat{M}_{23}^{(in)}$. The kinematical conditions of a production process are such that each of the diagrams of $\hat{M}_{23}^{(in)}$ contains at least one connected sub-diagram with large momentum transfer. So that the factorization of the amplitude, Eq.2, is equivalent to the χ PT transition amplitude of Cohen et al. [2].

Now we turn to calculate the transition amplitude for the $pp \rightarrow pp\pi^0$ reaction. We use the χ PT pion-nucleon sector heavy-fermion formalism (HFF) Lagrangian of the form,

$$L = L^{(0)} + L^{(1)} + L^{(2)} , \quad (2)$$

where,

$$L^{(0)} = \frac{1}{2}[(\partial_\mu \pi)^2 - m^2 \pi^2] - \frac{1}{6F^2}[\pi^2(\partial_\mu \pi)^2 - (\pi \dot{\partial}_\mu \pi)^2] + N^\dagger(v\partial)N + \quad (3)$$

$$N^\dagger[-\frac{1}{4F^2}\tau\dot{\pi} \times (v\partial)\pi - \frac{g_A}{F}S^\mu b f \tau[\partial_\mu b f \pi + \frac{1}{6F^2}(\pi\pi\partial_\mu\pi - \partial_\mu\pi\pi^2)]N;$$

$$L^{(1)} = \frac{1}{2M}(v^\mu v^\nu - g^{\mu\nu})[N^\dagger\partial_\mu\partial_\nu]N + \frac{1}{4F^2}[iN^\dagger\tau\pi \times \partial_\mu\pi\partial_\nu N + h.c.] \quad (4)$$

$$+ \frac{1}{2MF^2}N^\dagger[(c'_2 - \frac{g_A^2}{4})(v\partial\pi)^2 - c'_3(\partial_\mu\pi)^2 - 2c'_1m^2\pi^2] + \dots ,$$

and

$$L^{(2)} = -\frac{d_1}{MF}[iN^\dagger\tau(v\partial\pi)S^\mu\partial_\mu NN^\dagger N + h.c.] + \dots . \quad (5)$$

Here π and N are the pion and nucleon fields, v^μ is the nucleon four velocity, $(v\partial) = v^\mu\partial_\mu$ and, c'_1 , c'_2 and c'_3 denote the dimensionless low energy coupling constants. These are determined from fitting S-wave π^0N scattering data to be [8], $c'_1 = -1.63$, $c'_2 = 6.20$ and $c'_3 = -9.86$. To obtain the π production amplitude to order $D = 2$ one has to include, in addition to the tree diagrams, one loop diagrams with vertices from $L^{(0)}$. The main contributions to $M^{(in)}$ are

due to the diagrams of Fig. 1. The graphs 1a and 1b are the usual impulse and rescattering diagrams. Both are taken into account by Park et al. [1] and Cohen et al. [2]. The two graphs 1c and 1d which correspond to two-pion t-channel exchange having isoscalar-scalar quantum numbers, yield a substantial contribution to the amplitude. This is an analogous contribution to that from the t-pole σ -meson exchange (Fig. 2d and its cross counterpart) of the OBE model of Ref. [5]. Albeit, the sum of graphs 1a-1d is equivalent to the off mass-shell $T(\pi^0 p \rightarrow \pi^0 p)$ amplitude (Fig. 2a).

The other graphs 1e and 1f are contributions specific to the production process only and can not be reduced to one-pion exchanges. In Fig. 1e, the quantum numbers in the $N\bar{N} \rightarrow N\bar{N}\pi$ channel correspond to an isoscalar-scalar state. Like the graphs in Figs. 1c-1d, this diagram simulates the effective σ -meson exchange of the OBE model but with short range $\sigma p \rightarrow \pi^0 p$ production amplitude. The graph 1f is a short-range interaction mechanism provided by $L^{(2)}$.

The sum of all contributions from the graphs of Fig. 1 can now be written as,

$$M^{(in)}(pp \rightarrow pp\pi^0) = M_P^{(1)} + M_R^{(1)} + M_L^{(1)} + M_L^{(2)} + M_S^{(2)}. \quad (6)$$

where,

$$M_P^{(1)} = -i \frac{g_A^3}{8MF^3(Q^2 - m^2)} \mathbf{Q}^2 \mathbf{p} \sigma_1 + [1 \leftrightarrow 2, 3 \leftrightarrow 4], \quad (7)$$

$$M_R^{(1)} = i \frac{g_A}{2MF^3(Q^2 - m^2)} [(c'_2 + c'_3 - \frac{g_A^2}{4})mQ^0 - 2c'_1 m^2] \mathbf{p} \sigma_1 + [1 \leftrightarrow 2, 3 \leftrightarrow 4]; \quad (8)$$

$$M_L^{(1)} = i \frac{g_A^3}{12F^5(Q^2 - m^2)} [6mQ^0 - 2Q^2 - \frac{5}{2}m^2] B(q^2) \mathbf{p} \sigma_1 + [1 \leftrightarrow 2, 3 \leftrightarrow 4]; \quad (9)$$

$$M_L^{(2)} = i \frac{g_A^3}{24F^5} B(q^2) \mathbf{p} \sigma_1 + [1 \leftrightarrow 2, 3 \leftrightarrow 4]; \quad (10)$$

$$M_S^{(2)} = i \frac{d_1 \omega}{2FM} \mathbf{p} \sigma_1 + [1 \leftrightarrow 2, 3 \leftrightarrow 4] , \quad (11)$$

where σ denote the usual Pauli matrices, F and g_A are the pion radiative decay and axial vector coupling constants. The quantities $M_P^{(1)}$, $M_R^{(1)}$, $M_L^{(1)}$ denote one-pion exchange pole, rescattering and one-loop contributions, and $M_L^{(2)}$ and $M_S^{(2)}$ are contributions from graphs 2e and 2f. In Eqns.6-11, $p = (E = M + \mathbf{p}^2/2M, \mathbf{p})$ and $k = (\sqrt{m^2 + \mathbf{k}^2/2M}, \mathbf{k})$ stand for the center of mass (CM) four momenta of the incoming proton and pion produced;

$Q = (Q^0 = \mathbf{p}^2/2M, \mathbf{p})$ and $q = (\mathbf{p}^2/2M, \mathbf{p})$ are the transferred four momenta. The bracket $[1 \leftrightarrow 2, 3 \leftrightarrow 4]$ represents the contributions from the same diagram with the proton momenta p_1, p_3 interchanged with p_2, p_4 , respectively. The loop function is given by [8],

$$B(q^2) = (-3 + 2\mathbf{p}^2 \frac{d}{dq^2}) B_0(q^2), \quad (12)$$

$$B_0(q^2) = -\frac{1}{16\pi} \int_0^1 dz \sqrt{m^2 - q^2 z(1-z)}. \quad (13)$$

In the calculations to be presented below the values of constants and masses are taken to be: $F = 93.MeV$, $m = 135MeV$, $M = 938MeV$ and $g_A = 1.26$. There remains only one unknown constant, d_1 of Eqn. 5, to be determined. To do this we follow a similar procedure to that used in Refs. [8,2], i.e, assuming that the short-range interactions originate from ρ and ω vector meson exchanges only, and calculate these applying the covariant OBE model of Ref. [5]. This procedure yields,

$$d_1 = \frac{f_{\pi NN} F}{M} \left(\frac{g_{\rho NN}^2 (1 + \kappa)}{m_\rho^2 + Mm} + \frac{g_{\omega NN}^2}{m_\omega^2 + Mm} \right). \quad (14)$$

Here $m_\rho = 770MeV$, $m_\omega = 782MeV$ are the masses of the ρ and ω mesons, $f_{\pi NN}$ the πNN pseudovector coupling constants, $g_{\rho NN}$ and $g_{\omega NN}$ the ρNN and ωNN vector coupling constants and κ is the ratio of tensor to vector ρNN coupling constants. Their values are taken from Machleidt et al. [12].

Before presenting numerical results we make two remarks. The first is that the $\pi^0 p \rightarrow \pi^0 p$ elastic scattering amplitude is enhanced significantly because of offshellness and that the one-loop term $M_L^{(1)}$ depends strongly on the mass (Q^2) of the pion exchanged. At $Q = (m/2, \sqrt{Mm})$ it becomes sufficiently large so that the sum of $M_R^{(1)} + M_L^{(1)}$, although cancels in part by the $M_P^{(1)}$ term, can still make an important contribution to the $M^{(in)}(pp \rightarrow pp\pi^0)$. The second remark is concerned with the large momentum transfer through one-loop diagrams. At least one of the pion lines in a loop must have a large momentum ($\sim \sqrt{Mm}$) and therefore, this loop represents a mechanism which takes place over short distances. Since the loop terms dominate the production amplitude, then the $pp \rightarrow pp\pi^0$ reaction occurs mainly over short distances in full agreement with the results from OBE calculations

[5]. In fact there is a close correspondence between the different χ PT contributions and those of the OBE model. First, the overall contributions from the impulse and rescattering terms (diagrams 1a and 1b) is rather small [1,2] as suggested by OBE model [5] for the diagram 2a. Secondly, the main contribution to the production amplitude is due to the diagrams 1c and 1d which are the equivalent to contribution from diagram 2d. Thirdly, the contribution of the graph 2c and its cross diagram to the OBE model production amplitude are as negligibly small as the corresponding one-loop χ PT diagrams (not shown in Fig. 1). However, the OBE model calculations [5] do not account for the short range part of the $\sigma p \rightarrow \pi^0 p$ amplitude corresponding to the contribution of diagram 1e.

Our predictions for the cross section are presented in Figs. 3-4 along with the data of Refs. [13,14]. All curves are corrected for FSI following the procedure described in Ref. [5]. The dash-dotted curve displays our results with all of the terms of Eqn. 6 included and agrees rather well with the results of our OBE model calculations [5] (given by the solid line). The curve χ PT2 gives the predictions without the short-range interaction term $M_S^{(2)}$ taken into account. This term interferes destructively with the loop terms and brings the calculated cross section to close agreement with data. The curve χ PT1 represents the results of Cohen et al. [2]. We may thus conclude that taking into account the contributions from one-loop diagrams to chiral order D=2, χ PT reproduces the cross section of the $pp \rightarrow pp\pi^0$ reaction. With one-loop contributions, there is a close correspondence between χ PT and the OBE model.

The calculations above can be improved by first including small $\sim 1/m$ correction terms, arising in HFF. The transferred momentum in the $pp \rightarrow pp\pi^0$ reaction is rather large and the convergence of the HFF expansion is still to be verified. Secondly, contributions from other degrees of freedom must be taken into account. Excitations from the Δ (1232 MeV) nucleon isobar may well contribute to any of the graphs Fig. 1a-1e. Also, the vector meson contributions can be included explicitly, perhaps by using more generalized χ PT. To go beyond that to allow for η -meson excitations would require a broken SU(3) symmetry flavor version of χ PT. The η -meson is a Goldstone boson and hence it must be treated

on the same footing as the pion. Finally, as we have already indicated, the contribution from D=2 loop diagrams has the same order of magnitude as those from the lower order terms. The contributions from the next D=3 chiral order diagrams must then be calculated in order to ascertain the convergence of the χ PT expansion. Rough estimates indicate that such contributions may modify the calculated cross section by a few tens of per cents.

Acknowledgments This work was supported in part by the Israel Ministry Of Absorption. We are indebted to Z. Melamed for assistance in computation.

REFERENCES

- [1] B.-Y.Park et al., Phys. Rev. **C53** (1996) 1519.
- [2] T.D.Cohen et al., Phys. Rev. **C53** (1996) 2661.
- [3] T.S.H.Lee and D.Riska, Phys. Rev. Lett. **70**(1993) 2237.
- [4] C.J.Horowitz et al., Phys. Rev. **C49** (1994) 1337.
- [5] E.Gedalin, A.Moalem and L.Razdolskaja, nucl-th/9611005.
- [6] T.S.Park, D.-P.Min and M.Rho, Phys. Rep. **233**(1993) 341.
- [7] V.Bernard, N.Kaiser, T.-S.H.Lee, and Ulf-G.Meissner, Phys. Rep. **246**(1994) 315.
- [8] V.Bernard, N.Kaiser and Ulf-G.Meissner, Int. J. Mod. Phys. **E4** (1995) 193.
- [9] A.Moalem, L.Razdolskaja and E.Gedalin, hep-ph/9505264;
A. Moalem, E.Gedalin, L.Razdolskaja and Z.Shorer, π N Newsletter Proceeding of the
6th International Symposium on Meson-Nucleon Physics and the Structure of the Nu-
cleon, **10** (1995) 172.
- [10] A.Moalem, E.Gedalin, L.Razdolskaja and Z. Shorer, Nucl. Phys. **A589** (1995) 649;
A. Moalem, E.Gedalin, L.Razdolskaja and Z.Shorer, Nucl. Phys. **A600** (1996) 445.
- [11] S.Weinberg, Phys. Lett. **B251** (1990) 288; *ibid* **B295** (1992) 114.
- [12] R.Machleidt et al., Physics Reports **149** (1987) 1.
- [13] A.Bondar et al., Phys. Lett. **B356** (1995) 8.
- [14] H.O.Meyer et al., Nucl. Phys. **A539** (1992) 683.

Figure captions

FIGURES

FIG. 1. The χ PT diagrams giving the main contribution to the primary production amplitude for the $NN \rightarrow NN\pi^0$ reaction.

FIG. 2. The OBE model diagrams contributing to the $\hat{M}_{23}^{(in)}$ for the $pp \rightarrow pp\pi^0$ reaction.

FIG. 3. Predictions for the total cross section of the $pp \rightarrow pp\pi^0$ reaction vs. Q_{cm} , the energy available in the center of mass system. The curve χ PT2 gives the predictions without the short-range interaction term and the dash-dotted curve displays our results with all contributions included. The curve χ PT1 represents the results of Cohen et al. [2]. Our OBE model predictions [5] are drawn as a solid curve. The data points are taken from Refs. [13,14].

FIG. 4. Predictions for the total cross section vs. η_{max} , the maximal available momentum of pion in the center of mass system.

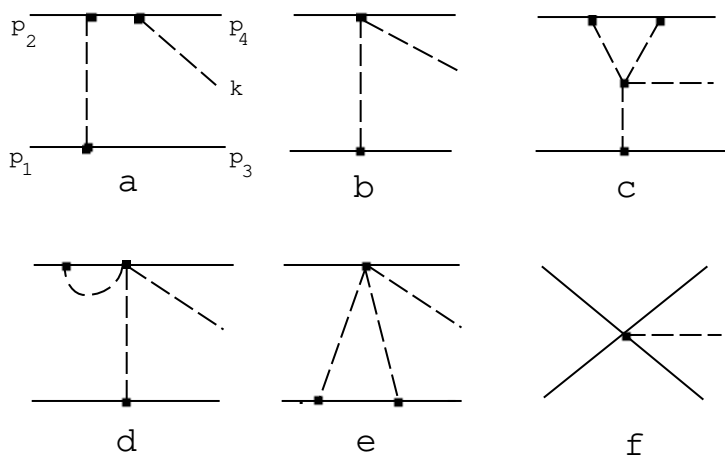


Fig.1

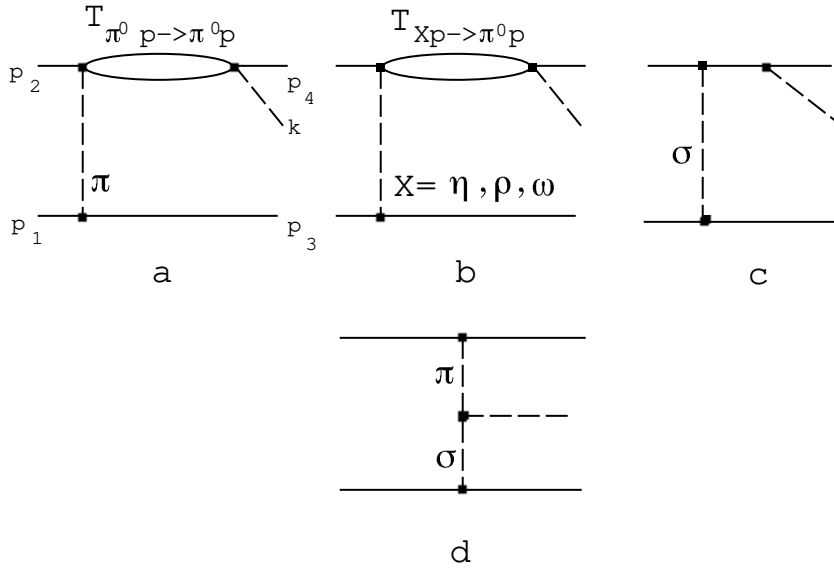


Fig.2

